



Molecular Crystals and Liquid Crystals Science and Technology. Section A. Molecular Crystals and Liquid Crystals

Publication details, including instructions for authors and
subscription information:

<http://www.tandfonline.com/loi/gmcl19>

Photoinduced Orientational Order in Dye-Doped Amorphous Polymeric Films

Michel Dumont^a

^a Institut d'Optique Théorique et Appliquée, Bât 503, BP 147,
91403, ORSAY cedex, France Fax:

Version of record first published: 24 Sep 2006.

To cite this article: Michel Dumont (1996): Photoinduced Orientational Order in Dye-Doped Amorphous Polymeric Films, Molecular Crystals and Liquid Crystals Science and Technology. Section A. Molecular Crystals and Liquid Crystals, 282:1, 437-450

To link to this article: <http://dx.doi.org/10.1080/10587259608037597>

PLEASE SCROLL DOWN FOR ARTICLE

Full terms and conditions of use: <http://www.tandfonline.com/page/terms-and-conditions>

This article may be used for research, teaching, and private study purposes. Any substantial or systematic reproduction, redistribution, reselling, loan, sub-licensing, systematic supply, or distribution in any form to anyone is expressly forbidden.

The publisher does not give any warranty express or implied or make any representation that the contents will be complete or accurate or up to date. The accuracy of any instructions, formulae, and drug doses should be independently verified with primary sources. The publisher shall not be liable for any loss, actions, claims, proceedings, demand, or costs or damages whatsoever or howsoever caused arising directly or indirectly in connection with or arising out of the use of this material.

PHOTOINDUCED ORIENTATIONAL ORDER IN DYE-DOPED AMORPHOUS POLYMERIC FILMS.

Michel DUMONT

Institut d'Optique Théorique et Appliquée, Bât 503, BP 147,
91403 ORSAY cedex, France, fax 33-1-69 41 31 92

Abstract This paper is a review of optical ordering processes in amorphous films containing photoisomerizable dye molecules. Photoinduced Anisotropy (PIA), Photoassisted Poling (PAP) and All-Optical Poling (AOP) are demonstrated through basic experiments and interpreted by a common theoretical model.

1. INTRODUCTION

Dye molecules (and particularly azo-dyes) are well known for their properties of photochromism and of anisotropy. *Photoinduced anisotropy* (PIA) has been studied for a long time, in viscous liquids and in polymeric films¹. In the last ten years a large interest has been focused on this family of molecules in all possible environments, because of their potentialities for optoelectronic applications. PIA in polymer films has been first proposed for real time polarization holography^{2,3}, which could lead to image processing devices (e.g. correlators) and which needs high molecular mobility. On the other hand, data storage⁴ requires high stability of the molecular order and the possibility of erasing and rewriting information. Substituted azo dyes, with an electron donor group (such as NH₂ or NRR') and an acceptor group (such as NO₂), are strongly polar and optically nonlinear. Polymer films doped with these molecules can be poled by heating them around the glass transition temperature (T_g) in the presence of a DC electric field which is then maintained while the sample is cooled down to room temperature. The molecular order created at T_g is frozen and the sample keeps a large $\chi^{(2)}$, leading to electrooptic applications, such as waveguide modulators, or second harmonic generation (although major problems are not yet efficiently solved for SHG: reabsorption of 2ω , phase matching and stability). This is *Thermally-Assisted Poling* (TAP)⁵.

Recently, two optical poling techniques have been demonstrated, at room temperature : first, *Photo-Assisted Poling*⁶ (PAP), in which the order is created by a DC field, like in TAP, but in which the viscosity of the polymer is overcome by optical pumping (through photoisomerization). PAP allows patterning of $\chi^{(2)}$, since only the illuminated areas are poled (e.g. alternate poling for SHG by quasi-phase matching). Second, *All-Optical Poling*^{7,8} (AOP, also named "seeding"), in which a non-centrosymmetric order

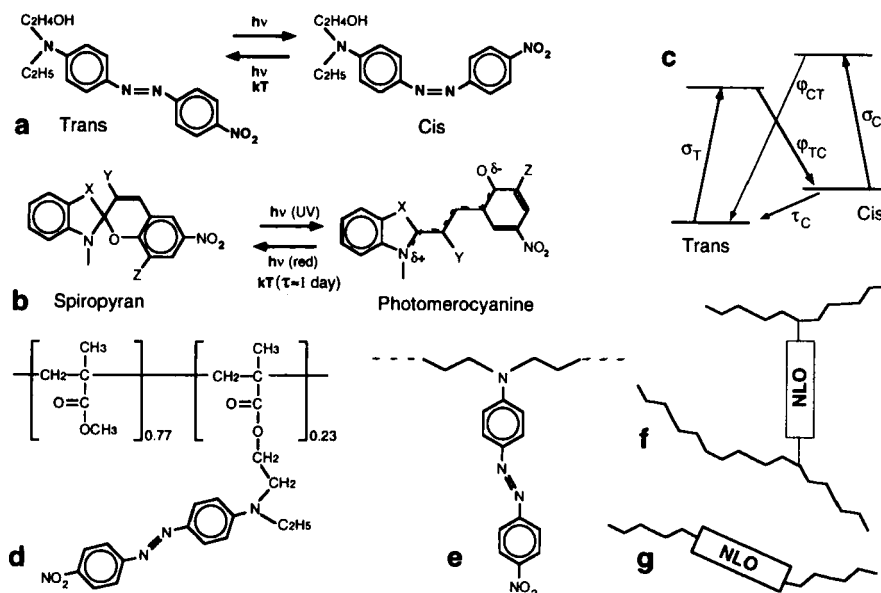


FIGURE 1. **a**: Photoisomerization of Disperse Red 1 (DR1). **b**: Spiropyran-merocyanine. **c**: Simplified diagram of azo-dyes levels. The reverse optical pumping (cis \rightarrow trans) also exists. **d**: PMMA-DR1 copolymer used in experiments described below. Pendant radicals have a large degree of freedom owing to the CH_2 spacers. **e**: the link to the polymer chain is stronger. **f** (cross-linking) and **g** (chromophores in the main chain) are structures used to stabilize the poling performed at $T \approx T_g$.

is created by the interference of a strong laser beam and its second harmonic. AOP has the advantage of producing automatic phase matching for SHG in thick samples and of allowing the orientation of molecules without dipole moment (octupolar molecules)⁹.

A large effort of research has been developed for designing efficient materials. The choice of active molecules¹⁰ is the first step, but the choice of the environment is probably more critical for practical applications. The main goal is to fit the molecular mobility to the various applications. For stable $\chi^{(2)}$ materials several routes have been explored: high T_g polymers, copolymers incorporating active molecules as pendant radicals or in the main chain, cross linking of dyes after poling... (Fig. 1). On the opposite, plasticizers are added in photorefractive polymers¹¹ in order to increase dyes mobility. Beside polymers, hybrid organic-inorganic materials (sol-gels) begin to be used^{12,13}.

In amorphous materials dye molecules are assumed to move independently from each other. At high concentration, chromophores may aggregate but in general they lose their optical properties. The orientational behavior is quite different in mesogenic materials, such as dye-doped liquid crystals (LC)³⁷. This is also the case of LC polymers in which azo-dye pendant side groups are linked to the polymer chain in alternation with mesogenic groups^{14,15}. The optically induced rotation of dye molecules drives a collective rotation of the whole LC, which can lead to optically switched LC devices.

Cooperative effects have been also observed in Langmuir-Blodgett (LB) films constituted of azo-dyes which are mesogenic by themselves¹⁶. These LB films can be used as anchoring surfaces for LC cells¹⁷: a preliminary illumination of LB coated surfaces determines easy axes for nematic LC. Azo dye LB films without intrinsic collective effect have been used for the optical command of LC cells¹⁸. Like in polymeric environment, the photoinduced rotation of dye molecules is most often based on photoisomerization, but collective effects modify deeply the dynamics of rotation and the competition between optical ordering and other anisotropic effects (such as surface effects) leads to more complicated structures (often biaxial).

In this paper we will focus our interest on photoinduced ordering processes in amorphous matrices. We will show that PIA, PAP and AOP can be described by a single model and differ only by the geometry of optical pumping and the symmetry of reorientation processes.

2. PHOTOINDUCED ORDERING MECHANISMS.

The most efficient photochromic anisotropic molecules are azo dyes, characterized by a double bond $N=N$ between two phenyl rings¹⁹. They present two isomeric shapes: trans (the more stable one) and cis. DR1 (fig. 1.a) will be used as an example for describing orientational ordering of photoisomerizable molecules by a resonant pumping beam, but other photochromic molecules can be used, such as spiropyrans (fig. 1.b).

Angular Hole Burning (AHB). The delocalization of conjugated π electrons along the principal axis of azo dye molecules makes their polarizability strongly anisotropic ($\alpha_{//} \gg \alpha_{\perp}$ and $\sigma_{//} \gg \sigma_{\perp}$ for the absorption cross section of the π - π band). A linearly polarized light beam selectively pumps molecules parallel to its polarization (probability $\propto \cos^2\theta$). As a part of excited trans molecules may relax to the ground state of the cis shape (Fig. 1.c), which has a long life time, optical pumping produces an anisotropic depletion of the angular distribution of trans : this is AHB. In the case of AOP, we will see that optical pumping contains a $\cos^3\theta$ term, producing a non-centrosymmetric AHB.

Angular Redistribution (AR). If AHB is the only mechanism, anisotropy disappears with the lifetime of cis, when the pump is switched off. Experimentally anisotropy has a longer life time (guest-host system) and can be permanent (with the copolymer of fig. 1d). This can be explained by a rotation of molecules in the trans-cis-trans photoisomerization cycle. This reorientation may occur by spontaneous rotation (thermal angular diffusion) during the lifetime of the cis state, which has a more spherical shape than the trans state, as many authors suggested it, but it is more likely to think that rotation is a consequence of the conformation changes in trans \rightarrow cis and cis \rightarrow trans isomerizations. When there is no external field (PIA and AOP), the rotation at each pumping cycle is

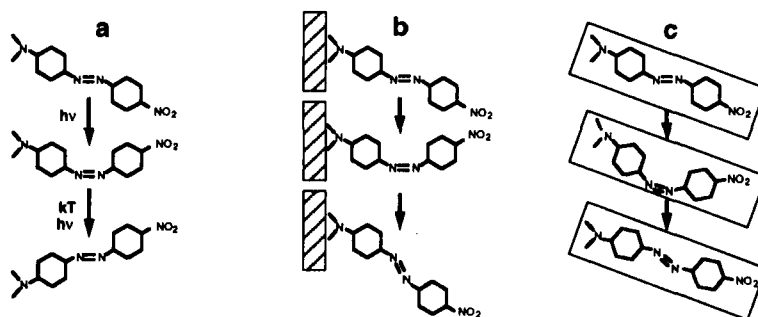


FIGURE 2. Rotation induced by photoisomerization of azo dyes. **a**: This scheme presented by many authors is not realistic since the $N=N$ double bond has no reason to remain fixed in space. **b**: A possible model when dye molecules are strongly linked to the polymer (fig. 1.e). **c**: The most realistic model: molecules are tightly caged in a small free volume. They progressively push the polymeric environment. Finally the rotation can be large, but needs a great number of cycles.

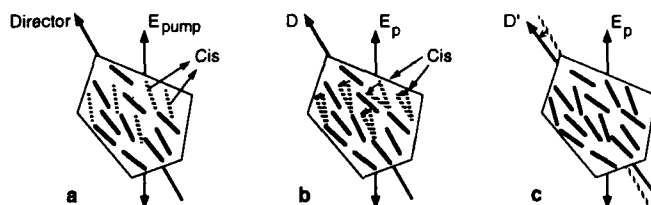


FIGURE 3. Cooperative effect: scheme of the three steps of the mechanism of rotation of the director of a LB domain, according to Palto *et al.*¹⁷. **a**: selective pumping of molecules doing the smallest angles with E_p . **b**: Relaxation of pumped molecules in the direction of the director. **c**: recrystallization with a titled director.

random and isotropic with respect to the initial direction in trans, but the result is an accumulation of molecules in the direction of smallest probability of pumping: AR amplifies and perpetuates the order created by hole burning. When there is a DC electric field (PAP), AR is no more isotropic: the torque on the dipole moment of molecules obliges them to rotate in the direction of the field, with some random thermal spreading.

Molecular environment is determinant for the stability of the photoinduced order, since it permits or not thermal diffusion in the trans state, when the pump is off. It is also determinant for the kinetics of AR induced by isomerization, as explained in fig. 2. The amplitude of the average rotation at each cycle depends on the free volume around each molecule and on its chemical links to the polymer chain (Van der Waals forces, H-bonds, covalent links, length of the spacer chain ... Fig 1d to g).

In the case of collective effects, like in LC polymers or in some LB films, Palto *et al.*¹⁶ gave another model: in each domain, the pumping is more efficient for molecules deviating from the director on the side of the distribution doing the smaller angle with the pump polarization (like in AHB), but AR tends to bring them back along the

director. The result is a small tilt of the director which slowly rotates away from the polarization of light (Fig. 3). Let us notice that isomerization is not necessary in this model (although it could increase the efficiency): when molecules on one side of the distribution are removed from the mesogenic state for a long time, remaining molecules tend to reorganize their average direction around a tilted director.

3. THEORETICAL MODEL.

3.1. General equations.

All ordering processes by optical pumping of photoisomerizable molecules can be represented by two rate equations coupling the angular distributions, $n_T(\Omega)$ and $n_C(\Omega)$ ($\Omega = \{\varphi, \theta, \xi\}$). T and C labels are used by reference to trans and cis states of azo dyes, but they can refer to the photoisomers of any other molecule. Equations include AHB ($\text{Pr}(\Omega)$ is the probability of optical pumping), AR (R_{TC} and R_{CT}) and diffusion²⁰⁻²²:

$$\frac{dn_T(\Omega)}{dt} = -\Phi_{TC} \text{Pr}(\Omega) n_T(\Omega) + \frac{1}{\tau_c} \int R_{CT}(\Omega' \rightarrow \Omega) n_C(\Omega') d\Omega' + \left(\frac{dn_T(\Omega)}{dt} \right)_{\text{Diff}} \quad (1-a)$$

$$\frac{dn_C(\Omega)}{dt} = \Phi_{TC} \int R_{TC}(\Omega' \rightarrow \Omega) \text{Pr}(\Omega') n_T(\Omega') d\Omega' - \frac{1}{\tau_c} n_C(\Omega) + \left(\frac{dn_C(\Omega)}{dt} \right)_{\text{Diff}} \quad (1-b)$$

The T-to-C pumping is made via short living excited levels, but we can neglect their population. Φ_{TC} is the quantum yield of isomerization (pumped molecules coming back directly to T are not observable, as far as they do not rotate). It would be easy to take into account the reverse C-to-T optical pumping by introducing a probability of leaving C and a redistribution on the arrival in T. All the ordering processes considered in this paper present an axial symmetry (fig.4). Therefore, the angular distribution of molecules does not depend on the azimuthal angle φ . In addition, the angle ξ is irrelevant if we assume that molecules have an axis of symmetry. For those reasons we will use the formalism of order parameters by projecting $n_T(\theta)$ and $n_C(\theta)$ on Legendre polynomials P_q :

$$n_T(\theta, \varphi) = \frac{1}{4\pi} \sum (2q+1) T_q P_q(\cos\theta) ; \quad n_C(\theta, \varphi) = \frac{1}{4\pi} \sum (2q+1) C_q P_q(\cos\theta) \quad (2)$$

The main interest of this formalism is that few parameters are needed for expressing the optical susceptibilities (parameters of parity $n+1$, up to $n+1$, for $\chi^{(n)}$ ²³ -cf. appendix 1). T_q and C_q are the usual normalized order parameters multiplied by the density of molecules in T or in C ($T_0 = N_T$ and $C_0 = N_C$ are the populations of T and C respectively).

3.2. Thermal Diffusion

In many materials, chromophores are free to rotate and their angular distribution spontaneously return to thermal equilibrium after any type of perturbation. It is the case of many guest-host systems at room temperature and of any material above T_g (TAP). This

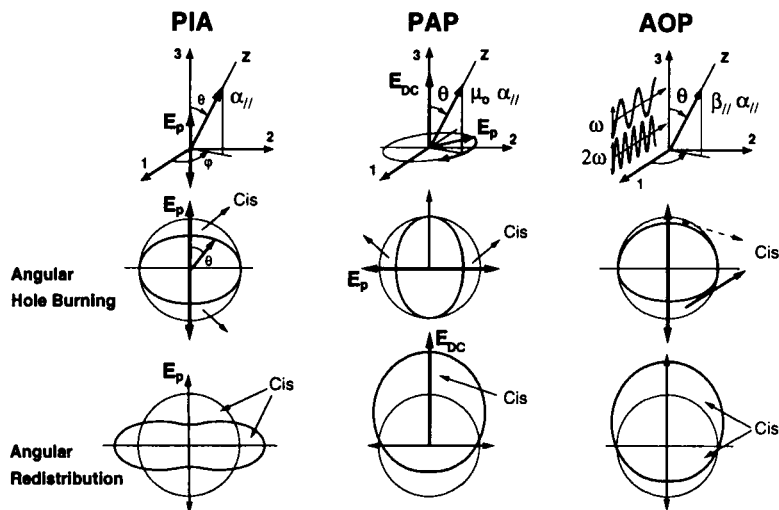


FIGURE 4. First line: Geometry of PIA, PAP and AOP. E_p is the polarization of the pumping light beam and Z the axis of a trans molecule. Second and third lines represent schematically the effect of hole burning and of angular redistribution on the angular distribution, $n_T(\theta, \varphi)$ (which is independent of φ). In PAP, poling is due to AR in a DC field, while in AOP it is due to non-centrosymmetric optical pumping.

process is usually represented by a diffusion equation, which has been developed for the Brownian motion in viscous liquids. In polymers, the validity of this model is highly questionable but it is the only simple mathematical expression of thermalization. In the presence of a DC electric field, E , the thermal diffusion equation for $n(\theta, t)$ is:

$$\frac{\partial n}{\partial t} = \left(D \Delta n - \frac{1}{\zeta} \vec{\nabla} \cdot (n \vec{\nabla}(U)) \right) = \frac{D}{\sin \theta} \frac{\partial}{\partial \theta} \left[\sin \theta \left(\frac{\partial n}{\partial \theta} + n \frac{\mu_0 E}{kT} \frac{\partial \cos \theta}{\partial \theta} \right) \right] \quad (3)$$

$D = kT/\zeta$ is the diffusion constant (k : Boltzmann constant; ζ : orientational viscosity) and $U = -\mu_0 E \cos \theta$ is the energy of the permanent dipole μ_0 in the electric field. The energy of the induced dipole, $(\alpha_{||} - \alpha_{\perp})E^2$, is assumed to be negligible. According to Benoit²⁴ the projection of eq.(3) on Legendre polynomials gives (order parameters: A_q):

$$\frac{dA_q}{dt} = -q(q+1) D \left[A_q + \frac{X}{2q+1} (A_{q+1} - A_{q-1}) \right]; \quad \text{with: } X = \frac{\mu_0 E}{kT} \quad (4)$$

The torque on dipoles introduces a coupling $\Delta q = \pm 1$ between order parameters which is responsible for the thermal poling, when the viscosity is not infinite. The stationary solution of eq. (4) is the thermal equilibrium depending only on X ($n(\theta, \varphi) \propto e^{X \cos \theta}$). In terms of order parameters, the rigorous solution is $A_q/A_0 = i_q(X)/i_0(X)$, where i_q is the spherical modified Bessel function of order q ²⁵. The transient behavior of A_q cannot be expressed rigorously but a very good approximation can be obtained by neglecting all A_q with q higher than q_m . Benoit²⁴ chose $q_m = 2$ in order to get only two equations (A_1

and A_2), leading to a two-exponential solution. This approximation is reasonable for $X < 1$ (valid in many experimental cases). For higher values of X , higher q_m are needed and a q_m -exponential solution can be obtained numerically.

When there is no DC field, this formalism leads to a simple exponential relaxation for each order parameter ($\tau_q = [D q(q+1)]^{-1}$). In practice, experimental observations show non-exponential decays. This behavior is usually explained by the inhomogeneity of the polymer in which each chromophore has a different free volume and consequently a different diffusion constant. The exponential behavior has to be averaged on the distribution of D values, but this distribution is unknown. Many authors represent experimental relaxations by a phenomenological stretched exponential, $\exp(-(t/\tau)^\beta)$, which is generally better than a bi- or a multi-exponential approximation. In addition it has been proved²⁷ that the time constants, τ_q , vary with time, after a perturbation which has affected the structure of the polymer (such as a temperature variation or optical pumping switching off). For the simplicity of algebra, we will use expression (3) and (4) for the diffusion terms in (1), but we will keep in mind the fact that the dispersion of the values of D (as well as that of τ_c) impedes any quantitative fitting of transients.

3.3. Equations for Order Parameters.

The projection of eqs.(1) on Legendre polynomials leads to a set of coupled equations:

$$\frac{dT_q}{dt} = -\sum_{q'} \text{Pr}_{qq'} T_{q'} + \frac{1}{\tau_c} \sum_{q'} R_{qq'}^{\text{CT}} C_{q'} - q(q+1) D_T \left[T_q + \frac{\mu_T E}{kT} \frac{(T_{q+1} - T_{q-1})}{2q+1} \right] \quad (5-a)$$

$$\frac{dC_q}{dt} = \sum_{q'q''} R_{qq'}^{\text{TC}} \text{Pr}_{q'q''} T_{q''} - \frac{1}{\tau_c} C_q - q(q+1) D_C \left[C_q + \frac{\mu_C E}{kT} \frac{(C_{q+1} - C_{q-1})}{2q+1} \right] \quad (5-b)$$

Selective Optical Pumping (AHB). According to the geometry of optical pumping, $\text{Pr}(\theta)$ can be expressed as a function of different powers of $u = \cos\theta$. In (5) it becomes the pumping matrix $\text{Pr}_{qq'}$ which couples order parameters. A term containing $\cos^p\theta$ involves the integral $\int_{-1}^1 P_q(u) u^p P_{q'}(u) du$ and introduces only couplings $\Delta q = \pm p; \pm p-2, \dots$. In PIA and in PAP (fig. 4), the pumping beam is linearly polarized (symmetry axis parallel to the polarization) or unpolarized (symmetry axis parallel to the propagation). A circularly polarized beam is equivalent to an unpolarized one, for non-chiral molecules. $\text{Pr}(\theta)$ is:

$$\text{Pr}(\theta)_{\text{lin}} = I_p \left(\sigma_{\perp} + (\sigma_{\parallel} - \sigma_{\perp}) \cos^2\theta \right) \quad \text{or} \quad \text{Pr}(\theta)_{\text{circ}} = I_p \left(\sigma_{\perp} + \frac{1}{2} (\sigma_{\parallel} - \sigma_{\perp}) \sin^2\theta \right) \quad (6)$$

I_p is the pump intensity. Introducing the average cross section and the anisotropy factor:

$$\bar{\sigma} = (\sigma_{\parallel} + 2\sigma_{\perp})/3 \quad ; \quad e = (\sigma_{\parallel} - \sigma_{\perp})/(\sigma_{\parallel} + 2\sigma_{\perp}) \quad (7)$$

and setting $\varepsilon=1$ for linear polarization and $\varepsilon=-1/2$ for circular polarization, one obtains:

$$\text{Pr}(\theta) = \bar{\sigma} I_p (1 + 2e\varepsilon P_2(\cos\theta)) \quad (8)$$

$$\begin{aligned} Pr_{qq} &= \bar{\sigma} I_p \Phi_{TC} (1 + 2\epsilon\epsilon q(q+1)(2q-1)^{-1}(2q+3)^{-1}) \\ Pr_{q,q\pm 2} &= 3\epsilon\epsilon \bar{\sigma} I_p \Phi_{TC} (q\pm 1)(q+1\pm 1)(2q+1\pm 2)^{-1}(2q+1)^{-1} \end{aligned} \quad (9)$$

The coupling $\Delta q = \pm 2$ creates all even orders, *i.e.* *alignment* of molecules, but this pumping is centrosymmetric.

In AOP, the two linearly polarized pump beams, at ω (strong) and 2ω (resonant), generate three pumping terms (appendix 2). The linear absorption at 2ω , expressed by (9), couples orders $\Delta q = \pm 2$. The two-photon absorption at ω introduces a pumping proportional to $\gamma_{//} I_\omega^2 \cos^4 \theta$ and couples $\Delta q = \pm 2, \pm 4$. Finally, the interference term:

$$Pr_{\text{seeding}} \propto \beta_{//} I_\omega \sqrt{I_{2\omega}} \cos^3 \theta \cos \phi \quad (10)$$

represents a non-centrosymmetric optical pumping which depends on the hyperpolarizability β of molecules and which introduces a coupling $\Delta q = \pm 1, \pm 3$. It produces a selective pumping of molecules oriented upward or downward, according to the relative phase ϕ of the two waves and it induces *orientation* of molecules. The pumping matrix from the two last terms are calculated with the help of relations:

$$\cos^3 \theta = \frac{1}{5} (3P_1(\cos \theta) + 2P_3(\cos \theta)); \quad \cos^4 \theta = \frac{1}{35} (7 + 20P_2(\cos \theta) + 8P_4(\cos \theta)) \quad (11)$$

$$\int_{-1}^1 P_q(u) P_k(u) P_{q'}(u) du = 2(2q'+1)^{-1} \langle qk00|q'0 \rangle^2 \quad (12)$$

$\langle qk00|q'0 \rangle$ is a Clebsch-Gordan coefficient ($\neq 0$ if $|q-k| \leq q' \leq q+k$ and if $q+k+q'$ is even).

Angular Redistribution (AR). The most difficult problem is the choice of a model for AR during the transition from one isomeric form to the other. The model must represent a statistical spreading of the angular distribution and the tendency for permanent dipoles to be oriented in the direction of the electric field, if there is one. For those reasons, we calculate the rotation matrices $R_{qq'}^{TC}$ and $R_{qq'}^{CT}$ with a phenomenological diffusion model (like in §3.2), in a fictitious intermediate state²². This model is thermodynamically correct and depends only on two adjustable parameters, $X^* = \mu_0 E / kT^*$, where T^* is a virtual temperature, which characterizes the competition between the ordering torque (if $E \neq 0$, *i.e.* for PAP) and the disordering thermal spreading of the distribution, and $D^* \tau^*$, the product of a virtual diffusion constant by the time spent in the virtual state. This last parameter measures the average rotation in each elementary process, or, in other words, the loss of memory of the initial orientation ($D^* \tau^* \ll 1$ means a very small rotation at each isomerization and $D^* \tau^* \gg 1$, the total completion of the thermal equilibrium in the virtual state *i.e.* thermal poling, if $E \neq 0$, or complete disorientation, if $E = 0$).

For PIA and AOP ($E = 0$), $R_{qq'}^{TC}$ and $R_{qq'}^{CT}$ are diagonal and cannot create order: they can only destroy it. Diagonal elements are $\exp\{-q(q+1)(D^* \tau^*)_{TC \text{ or } CT}\}$. The fact that these matrices are diagonal, if $E = 0$, is more general than this special model. It means that redistribution is isotropic around the initial orientation and that the probability of

rotation depends only on the absolute value of the rotation angle $\alpha = \{\theta', \varphi'\} - \{\theta, \varphi\}$, but not on the initial or the final orientations. It can be demonstrated that R_{qq}^{TC} and R_{qq}^{CT} are the projections of $R_{TC}(\alpha)$ and $R_{CT}(\alpha)$ on the Legendre polynomial $P_q(\cos\alpha)$ ²⁰.

Resolution of equations (5) ^{21,22} : They are reduced to a finite set of coupled equations by neglecting T_q and C_q for q larger than q_m , which is chosen large enough to keep a good accuracy up to $q=4$ (for calculation up to $\chi^{(3)}$). The solution of the system of $2q_m+1$ equations is a sum of $2q_m+1$ exponentials which are computed numerically.

4. SOME EXPERIMENTAL RESULTS.

4.1. Probing Techniques.

Dichroism measurement (Fig. 5) is the simplest method for probing photoinduced anisotropy. Polymer films, deposited on a glass slide, are pumped by a linearly polarized beam. The absorbance [$A = \ln(I_0/I_t)$] is measured for parallel and perpendicular polarizations, when the pump is switched on and off. One obtains ($\delta\sigma = \sigma_{//} - \sigma_{\perp}$):

$$A_m = \frac{1}{3}(A_{//} + 2A_{\perp}) = \bar{\sigma}_T T_0 + \bar{\sigma}_C C_0 \quad ; \quad A_{//} - A_{\perp} = \delta\sigma_T T_2 + \delta\sigma_C C_2 \quad (13)$$

Attenuated Total Reflection (ATR) ^{28,29} (fig. 6) is a powerful method, since it permits the measurement of the thickness of the film and of the index of refraction in the three principal directions (n_z perpendicular to the film, n_x in the plane of incidence). PIA is studied by measuring the variations Δn_x , Δn_y and Δn_z , induced by a polarized pump beam. Electrooptic effects are measured by applying a modulated voltage, V_{Ω} , on the top electrode and by measuring modulations of the reflectivity. The Pockels coefficients are:

$$r_{i3} = -2n_i^{-4} \chi_{i33}^{(2)}(-\omega; \omega, 0) = -2n_i^{-3} \Delta n_i(\Omega) h/V_{\Omega} \quad (i = 1, 3) \quad (14)$$

$z \equiv 3$ is the poling axis and h is the thickness of the film (1 to 2 μm). The measurement of Δh gives the piezoelectricity of the film. It is important to measure it, since piezoelectricity produces an indirect electrooptic effect (via photoelasticity) which is difficult to distinguish from the direct electronic Pockels effect ²⁹. With DR1, this correction is small. For PAP, a DC field, E_0 , is added to E_{Ω} and the film is pumped with a circularly polarized beam, through one of the semi-transparent electrodes. One can observe the dynamics of poling by recording the modulation of the reflectivity near the TM mode of largest incidence. The signal is approximately proportional to the modulation of Δn_z :

$$\begin{aligned} 2n_z \Delta n_z &= 2\chi_{333}^{(2)}(E_0 + E_{\Omega} \cos \Omega t) + 3\chi_{3333}^{(3)}(E_0 + E_{\Omega} \cos \Omega t)^2 \\ &= (2\chi_{333}^{(2)} + 6\chi_{3333}^{(3)} E_0) E_{\Omega} \cos \Omega t + \frac{3}{2} \chi_{3333}^{(3)} E_{\Omega}^2 \cos 2\Omega t + \dots \end{aligned} \quad (15)$$

The modulation at 2Ω gives $\chi^{(3)}$, which always exists. $\chi^{(3)} E_0$ is then extracted from the modulation at Ω , in order to obtain $\chi^{(2)}$ which characterizes the poling of the film.

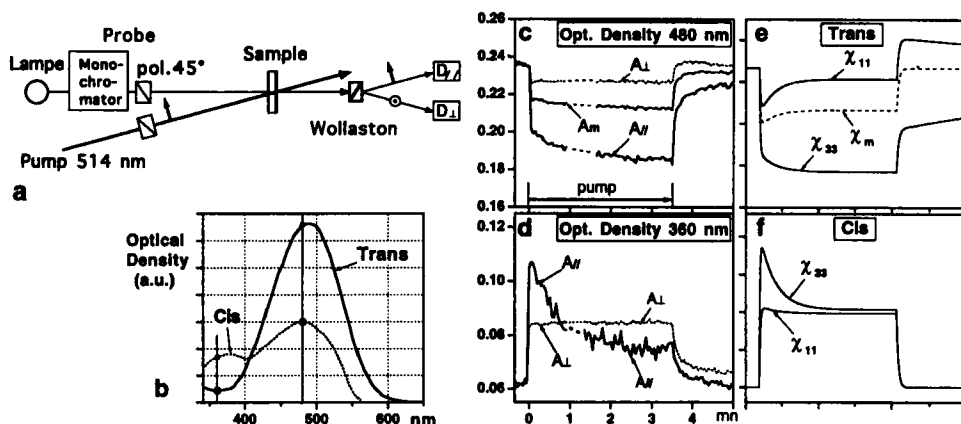


FIGURE 5. a: Dichroism experiment. b: Absorption spectrum of trans and cis states of DR1³⁰. c, d: Record of the optical density for both polarizations, at 480 nm (more sensitive to trans. Pumping by the probe slightly distorts this curve) and at 360 nm (more sensitive to cis). e, f: Theoretical simulation of $\chi^{(1)}$.²²

Ellipsometry^{31,32} gives the same kind of measurements: it is often easier experimentally than ATR, but the analysis of data is more difficult if accuracy is needed. $\chi^{(2)}$ can be also measured by second harmonic generation in a film submitted to optical pumping under a corona discharge^{33,34}. The SHG tensor, $d_{3j} = \frac{1}{2} \chi_{3ij}^{(2)}(-2\omega; \omega, \omega)$, is estimated by Maker fringes technique, but this method is not very accurate and is often based on the assumption that $A_3 \ll A_1$ ($d_{33} = 3d_{31}$), which is true for a low poling.

4.2. Photoinduced anisotropy (PIA).

When the linearly polarized pump is switched on, Δn_{\perp} and ΔA_{\perp} always begin to decrease with a slope which is one third of that of Δn_{\parallel} and ΔA_{\parallel} , as predicted by hole burning theory (with pure AHB - *i. e.* without AR - $n_T(\theta)$ and order parameters can be rigorously calculated²¹). But after some time the angular redistribution tends to increase Δn_{\perp} and ΔA_{\perp} . Their final sign, as well as the time needed to reach the stationary state, depend on the pump intensity and on the average rotation at each pumping cycle²⁰. With DR1-PMMA copolymer the reorientation is slow (small rotation at each cycle) but a large permanent anisotropy is obtained. This anisotropy can be rewritten in another direction by a new pumping²¹. When the pump is switched off, ΔA_m (or Δn_m) rapidly recovers its initial value, which proves the absence of photochemical degradation of DR1.

Fig. 5 shows dichroism experiments on PMMA-DR1 copolymer diluted in PMMA in order to reduce the optical density (the stability of anisotropy is also reduced). With a probe at $\lambda = 480$ nm, for which $\sigma_T \approx 2.5 \sigma_C$, one has $A_{\parallel} < A_{\perp}$ and the signal reasonably looks like the calculated evolution of $\chi^{(1)}$ in trans²². More interesting is the dichroism measured with a probe at $\lambda = 360$ nm, which is more sensitive to the cis state: absorption increases for both polarizations and ΔA_{\parallel} is twice ΔA_{\perp} , at the beginning, but decreases and becomes smaller than ΔA_{\perp} after ~50 s. This inversion of the anisotropy is explained

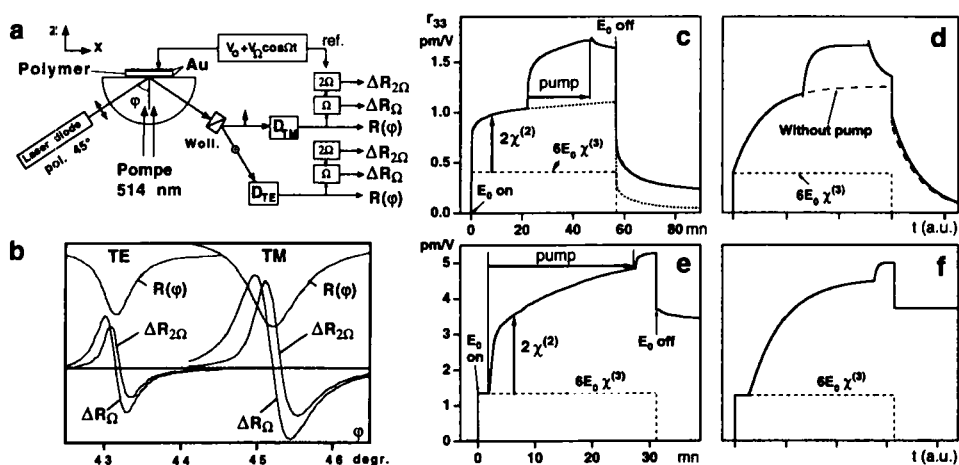


FIGURE 6. **a**: ATR experiment^{28,29}. The polymer film is spin coated on a glass plate previously covered with a thin metallic layer and which is put in contact with a half sphere, through which the reflectivity of the sample is recorded as a function of the incidence angle, for polarizations TM and TE. The position of dips gives the three indices and the thickness of the film. A modulated voltage applied to the top electrode ($\Omega \approx 1\text{ kHz}$) and lock-in detections give Pockels, piezoelectric (at Ω), Kerr and electrostriction effects (2Ω). A DC voltage is applied for poling. **b**: An example of experimental curves. **c** to **f**: Photoassisted poling of a PMMA-DR1 guest-host film (**c**) and a copolymer (**e**) from ref. 6. Experimental curves (r_{33}) represent the modulated term at Ω in (15). **d** and **f** are the corresponding calculated curves (from ref 22); they differ mainly by the diffusion in trans. The increase of r_{33} when the pump is switched off is due to oriented cis molecules coming back in trans.

by the evolution of $\chi^{(1)}$ in cis: first, AHB dominates and molecules parallel to the pump polarization are transferred from trans to cis, but slowly AR increases the anisotropy in trans and erases it in cis (there is no more parallel molecules to be pumped). This behavior proves two important features: (1) AR is slow (small rotation at each optical pumping cycle); (2) the transition dipole moment in cis is almost parallel to that in trans before photoisomerization.

4.3. Photoassisted Poling (PAP).

PAP has been observed as well by ATR⁶ as by SHG³³. With guest-host DR1-PMMA, a partial orientation is obtained at room temperature by action of the DC field alone, but orientation is increased by optical pumping (fig. 6.c). The relaxation after the removal of the field is much faster in the absence of optical pumping but in both cases it is complete after a few hours. With the copolymer (fig. 1 d) there is almost no rotation without optical pumping and PAP produces a permanent poling (fig. 6.e). The general behavior has been correctly simulated in both cases (fig. 6.d & e)²² but the shape of transient curves is not accurately represented since we use monoexponential relaxations. As explained in § 3.2, there is a wide dispersion of diffusion constants, from one chromophore to another, and we should have mix “fast” and “slow” molecules in our theoretical model.

Owing to the short lifetime of the *cis* state, it is difficult to determine at which step of the cycle DR1 does rotate. As far as rotation is small at each optical pumping cycle, the result is almost the same if rotation occurs either in the *trans*–*cis* photoisomerization, or during the *cis* lifetime, or in the *cis*–*trans* thermal relaxation. On the opposite, with spiropyran, photomerocyanine, obtained by UV pumping, has a long lifetime and ATR measurements are sensitive to merocyanine only. By applying the DC field during or after the optical pumping period, a large difference of poling has been observed^{22,34}: AR induced by photoisomerization is more efficient than thermal diffusion of the photoisomer after it has been created. Let's notice that merocyanine is longer than spiropyran, while *cis* DR1 is shorter than *trans*: we must not generalize the above conclusion, but we have proved that rotation can be associated with photoisomerization processes. The same experiments also demonstrated that rotational mobility slowly decreases, on hours time scale, after the end of optical pumping, in agreement with Bauer *et al.* results²⁷.

Some authors²⁷ compared the efficiency of thermal poling and of optical poling. They found better results with thermal poling, as well for the final electrooptic coefficient as for its long term stability. The first limitation seems to be the small penetration depth of the pumping light, in high concentration films²⁷. The second limitation is probably that a proportion of molecules has a too small mobility to be oriented in a reasonable time. Nevertheless, we have some experimental proofs that, after optimization, the poling limit could be better by optical means.

4.4. All-Optical Poling (AOP).^{7-9,36}

DR1-doped films were irradiated by a pulsed Nd-YAG laser beam and its second harmonic (seeding). Periodically the incident 2ω beam was interrupted and SHG was measured, in order to estimate the degree of poling of the sample. Like in PAP, the copolymer led to higher and much more stable poling than guest-host. The $\cos\phi$ dependence, in (10), has been demonstrated, as well as the competition between poling by the interference term and one- and two-photon pumping. C. Fiorini³⁶ used a model very similar to the above one to calculate the poling efficiency as a function of $I_{2\omega}/I_\omega$ and obtained a qualitative agreement with experiments. Octupolar molecules have been oriented⁹, but in this case photoisomerization didn't exist and poling was due to another mechanism.

5. CONCLUSION.

The formalism presented in this paper is suitable for any type of optical angular hole burning followed by some rotation of molecules, eventually in the presence of a DC field, provided there is no cooperative effect. It is particularly well adapted to photoisomerization of anisotropic molecules such as azo dyes or spiropyrans. It has been used successfully for understanding qualitatively all experimental features of PIA, AOP and PAP. The major remaining difficulty is the use of exponential decays for modeling re-

laxation processes. AOP and PAP induce a permanent poling at room temperature, in DR1-PMMA copolymer ($D_T=0$) and not in guest-host ($D_T \neq 0$), but the poling is slow (small rotation at each pumping cycle). A controversy remains: which rotation mechanism is the most efficient? diffusion in cis or angular redistribution induced by photoisomerization? With DR1, experiments cannot answer to this question. With spiropyran it has been shown that rotation does exist during the transition to photomerocyanine.

Appendix 1.

Assuming axial symmetry of molecules ($\alpha_{xx}=\alpha_{yy}=\alpha_{\perp}$ and $\beta_{zz}=\beta_{yy}=\beta_{\perp}$) and of the angular distribution (axis 3) and A_q being the order parameters defined in (2), one has:

$$\chi_{33}^{(1)} = \frac{1}{3} [A_0(\alpha_{//} + 2\alpha_{\perp}) + 2A_2(\alpha_{//} - \alpha_{\perp})]; \chi_{11}^{(1)} = \chi_{22}^{(1)} = \frac{1}{3} [A_0(\alpha_{//} + 2\alpha_{\perp}) - A_2(\alpha_{//} - \alpha_{\perp})]$$

$$\chi_{33}^{(2)} = \frac{1}{3} [3A_1(\beta_{//} + 2\beta_{\perp}) + 2A_3(\beta_{//} - 3\beta_{\perp})]; \chi_{31}^{(2)} = \chi_{32}^{(2)} = \frac{1}{3} [A_1(\beta_{//} + 2\beta_{\perp}) - A_3(\beta_{//} - 3\beta_{\perp})]$$

Appendix 2. Pumping probability in AOP.

As shown by Charra *et al.* ⁷, for a transition $T \rightarrow e$ resonant at 2ω ($\omega_0 \approx 2\omega$), the amplitude of probability of excitation of molecules is (at second order of perturbation):

$$\langle e | \psi \rangle \propto \bar{\mu}_{Te} \cdot \bar{E}_{2\omega} + (\bar{\mu}_{Te} \cdot \bar{E}_{\omega})((\bar{\mu}_T - \bar{\mu}_e) \cdot \bar{E}_{\omega}) / (2\hbar(\omega_0 - \omega))$$

μ_{Te} is the transition dipole; μ_T and μ_e are the permanent dipoles in T and e. The probability of transition from T to e is proportional to $|\langle e | \psi \rangle|^2$:

$$\text{Pr}(T \rightarrow e) \propto |\bar{\mu}_{Te} \cdot \bar{E}_{2\omega}|^2 + \text{Re} \left\{ \frac{(\bar{\mu}_{Te}^* \cdot \bar{E}_{2\omega}^*)(\bar{\mu}_{Te} \cdot \bar{E}_{\omega})(\Delta \bar{\mu} \cdot \bar{E}_{\omega})}{\hbar(\omega_0 - \omega)} \right\} + \left| \frac{(\bar{\mu}_{Te} \cdot \bar{E}_{\omega})(\Delta \bar{\mu} \cdot \bar{E}_{\omega})}{2\hbar(\omega_0 - \omega)} \right|^2$$

The first term is linear absorption of 2ω ($\alpha \propto \mu_{Te} \otimes \mu_{Te}^*$). The second term is a new interference effect. By recombining matrix elements μ_{Te} and $\mu_T - \mu_e$ it can be written as $\beta : (\bar{E}_{2\omega}^* \bar{E}_{\omega} \bar{E}_{\omega})$ where $\beta \propto \mu_{Te}^* \otimes \mu_{Te} \otimes \Delta \mu$. For rod like molecules ($\beta_{\perp}=0$), if both beams are linearly polarized, one obtains (10). The last term represents the two-photon absorption at ω which can be written $\gamma_{//} I_{\omega}^2 \cos^4 \theta$ ($\gamma \propto |\mu_{Te} \otimes \Delta \mu|^2$ is the second order hyperpolarizability).

REFERENCES

1. B.S.Neporent, O.V.Stolbova: Opt. Spektrosk., **10**, 287 (1961) [Opt. Spectrosc., **10**, 146 (1961)]; Opt. Spektrosk., **14**, 624 (1963) [Opt. Spectrosc., **14**, 331 (1963)]. A.M.Makushenko, B.S. Neporent, O.V., Stolbova, Opt. Spektrosk., **31**, 557 (1971) [Opt. Spectrosc. **31**, 295 (1971)]; Opt. Spektrosk., **31**, 741 (1971) [Opt. Spectrosc. **31**, 397 (1971)];
2. T.Todorov, L.Nikolova, N.Tomova, Appl. Optics, **23**, 4309 (1984).
3. C. Solano, R.A. Lessard and P. Roberge, Applied Optics **26**, 1989 (1987) R.Lessard and J.J. Couture, Mol. Cryst. Liq. Cryst. **183**, 451 (1990)
4. P. Rochon, J. Gosselin, A. Natansohn and S. Xie, Appl. Phys. Lett. **60**, 4 (1992). A. Natansohn, P. Rochon, J. Gosselin and S. Xie, Macromolecules, **25**, 2268 (1992).
5. D.M. Burland, R.D. Miller and C. A. Walsh, Chem. Rev., **94**, 31 (1994).

6. Z. Sekkat and M. Dumont, Appl. Phys. B, **54**, 486 (1992).
7. Z. Sekkat and M. Dumont, Nonlinear Optics, **2**, 359 (1992).
7. F. Charra, F.Kajzar, J.M. Nunzi, P. Raimond, E. Idiart, Optics Lett., **18**, 941 (1993).
8. C. Fiorini, F. Charra, J.M. Nunzi and P. Raimond, Nonlinear Optics, **2**, 339 (1995)
- J.M. Nunzi, C. Fiorini, F. Charra, F.Kajzar and P. Raimond, in Polymer Thin Films for Photonics. ACS symposium series (1994).
9. J.M. Nunzi, F. Charra, C. Fiorini and J. Zyss, Chem. Phys. Lett., **219**, 349 (1994).
10. J. Zyss, I. Ledoux and J.F. Nicoud, in Molecular Nonlinear Optics, (Academic Press, New York, 1994), Chap4, pp. 129-200.
11. W.E. Moerner and S.M. Silence, Chem. Rev., **94**, 127 (1994).
12. P. Griesmar, C. Sanchez, G. Puccetti, I. Ledoux and J. Zyss, Molecular Engineering, **1**, 205 (1991).
13. F. Chaput, J.P. Boilot, D. Riehl and Y. Levy, in Sol-Gel Optics III, editor J.D. Mackenzie, SPIE proceedigs Vol 2288 (1994), pp. 286-297.
14. U. Weisner, M. Antonietti, C. Boeffel and H.W. Spiess, Makromol. Chem., **191**, 2133 (1990).
- U. Weisner, N. Reynlds, C. Boeffel and H.W. Spiess, Liquid Crystals, **11**, 251 (1992)
15. A. Petri, Ch. Bräuchle, H. Leigeberg, A. Miller, H.-P. Weitzel and F.-H. Kruezer, Liquid Crystals, **15**, 113 (1993).
- A. Petri, S. Kummer, H. Anneser, F. Feiner and Ch. Bräuchle, Ber. Bunsenges. Pys. Chem., **97**, 1281 (1993).
16. S.P. Palto, L.M. Blinov, S.G. Yudin, G. Grewer, M.Schönhoff and M. Lösche, Chem. Phys. Lett., **202**, 308 (1993).
17. S.P. Palto, S.G. Yudin, C. Germain and G. Durand, J. de Physique II, **5**, 133 (1995)
18. Z. Sekkat, M. Büchel, H. Knobloch, T. Seki, S. Ito, J. Koberstein and W. Knoll, Optics Comm., **111**, 324 (1994).
19. H. Rau, Photoisomerization of azobezenes, in "Photochemistry and Photophysics, Vol. II", J.F. Rabek, ed., CRC press, Boca Raton, Florida (1990) p. 119.
20. Z. Sekkat and M. Dumont, Synthetic metal, **54**, 373 (1993)
21. M. Dumont, S. Hosotte, G. Froc and Z. Sekkat, in Photopolymers and Applications in Holography, Optical Sensors and Interconnects, editor R. Lessard, SPIE proceedings 2042 (1993) p 2 .
22. M. Dumont, G.Froc and S.Hosotte, Nonlinear Optics, **9**, 327 (1995)
23. J. Le Grange, M.G.Kuzyk and K.D.Singer, Mol. Cryst. Liq. Cryst. **150b**, 567 (1987)
24. H. Benoit, Ann. Phys. (Paris), **6**, 561 (1951).
25. J.W. Wu, J. Opt. Soc. Am., **B8**, 142 (1991).
26. Z. Sekkat and W. Knoll, Ber. Bunsenges. Phys. Chem **98**, 1231 (1994).
27. S. Bauer-Gogonea, S. Bauer, W. Wirges and R. Gerhard-Multhaupt, J. Appl. Phys. **76**, 2627 (1994).
28. M. Dumont, Y. Levy and D. Morichière, in: Organic Molecules for Nonlinear Optics and Photonics, ed.: J.Messier, F.Kajzar and P.Prasad (Nato ASI Series vol. E 194, Kluwers, Dordrecht 1991), p461
29. M. Dumont, D. Morichère, Z. Sekkat and Y. Levy, in Photopolymer Device Physics, Chemistry, and Applications II, ed. R. Lessard, SPIE proceedings Vol 1559 (1991), p 127.
30. R. Loucif-Saïbi, K. Nakatani, J. Delaire, M. Dumont and Z. Sekkat, Chem. Mater. **5**, 229 (1993).
31. C.C. Teng and H.T. Man, Appl. Phys. Lett. **56**, 1734 (1990).
32. Y.Levy, M. Dumont, E. Chastaing, P. Robin, P.A. Chollet, G. Gadret and F. Kajzar, Nonlinear optics, **4**, 1 (1993)
33. M. Dumont, Z. Sekkat, R. Loucif-Saïbi, K. Nakatani and J. Delaire, Nonlinear Optics, **5**, 395(1993)
34. J.Delaire, Y.Atassi, R.Loucif-Saïbi and K.Nakatani, Nonlinear Optics, **9**, 317 (1995)
35. Y. Atassi, J. Delaire and K. Nakatani , J. Phys. Chem. (in press)
36. C. Fiorini, thesis, Université Paris XI, Orsay (1995).
37. For references on azo dyes in LC, see other papers in this issue, e.g. by I. Janossy